

Large mixing angles for neutrinos from infrared fixed points

J.A. Casas^{1,2*}, J.R. Espinosa^{2,3†} and I. Navarro^{4‡}

¹ IEM (CSIC), Serrano 123, 28006 Madrid, Spain

² IFT C-XVI, UAM., Cantoblanco, 28049 Madrid, Spain

³ IMAFF (CSIC), Serrano 113 bis, 28006 Madrid, Spain

⁴ IPPP, University of Durham, DH1 3LE, Durham, UK

Abstract

Radiative amplification of neutrino mixing angles may explain the large values required by solar and atmospheric neutrino oscillations. Implementation of such mechanism in the Standard Model and many of its extensions (including the Minimal Supersymmetric Standard Model) to amplify the solar angle, the atmospheric or both requires (at least two) quasi-degenerate neutrino masses, but is not always possible. When it is, it involves a fine-tuning between initial conditions and radiative corrections. In supersymmetric models with neutrino masses generated through the Kähler potential, neutrino mixing angles can easily be driven to large values at low energy as they approach infrared pseudo-fixed points at large mixing (in stark contrast with conventional scenarios, that have infrared pseudo-fixed points at zero mixing). In addition, quasi-degeneracy of neutrino masses is not always required.

June 2003

*E-mail: alberto@makoki.iem.csic.es

†E-mail: espinosa@makoki.iem.csic.es

‡E-mail: ignacio.navarro@durham.ac.uk

1 Introduction

The experimental study of flavour non-conservation in diverse types of neutrino fluxes (solar, atmospheric and "man-made") has produced in recent years considerable evidence in favour of oscillations among massive neutrinos [1]. Theoretically, the most economic scenario to accommodate the data (or at least the more firmly established data, therefore leaving aside the LSND anomaly [2]) assumes that the left-handed neutrinos of the Standard Model (SM) acquire Majorana masses through a dimension-5 operator [3], which is the low-energy trace of lepton-number violating physics at much higher energy scales (the simplest example being the see-saw [4]).

Neutrino masses are then described by a 3×3 mass matrix \mathcal{M}_ν that is diagonalized by the PMNS [1] unitary matrix V :

$$V^T \mathcal{M}_\nu V = \text{diag}(m_1, m_2, m_3) . \quad (1)$$

The masses m_i are real (not necessarily positive) numbers. Following a standard convention we denote by m_3 the most split eigenvalue and choose $|m_1| \leq |m_2|$. For later use we define the quantities

$$\Delta m_{ij}^2 \equiv m_i^2 - m_j^2 , \quad \Delta_{ij} \equiv \frac{m_i - m_j}{m_i + m_j} , \quad \nabla_{ij} \equiv \frac{m_i + m_j}{m_i - m_j} . \quad (2)$$

The latter plays an important rôle in the RG evolution of V . For simplicity we set CP-violating phases to zero throughout the paper, so V can be parametrized by three successive rotations as

$$V = R_{23}(\theta_1) R_{31}(\theta_2) R_{12}(\theta_3) = \begin{pmatrix} c_2 c_3 & c_2 s_3 & s_2 \\ -c_1 s_3 - s_1 s_2 c_3 & c_1 c_3 - s_1 s_2 s_3 & s_1 c_2 \\ s_1 s_3 - c_1 s_2 c_3 & -s_1 c_3 - c_1 s_2 s_3 & c_1 c_2 \end{pmatrix} , \quad (3)$$

where $s_i \equiv \sin \theta_i$, $c_i \equiv \cos \theta_i$.

The experimental information on the neutrino sector is the following. For the CHOOZ angle: $\sin^2 \theta_2 < 0.052$; for the atmospheric neutrino parameters: $1.5 \times 10^{-3} < \Delta m_{atm}^2 / \text{eV}^2 < 3.9 \times 10^{-3}$ and $0.45 < \tan^2 \theta_1 < 2.3$; and for the solar ones (with the MSW mechanism [5] at work): $5.4 \times 10^{-5} < \Delta m_{sol}^2 / \text{eV}^2 < 10^{-4}$ or $1.4 \times 10^{-4} < \Delta m_{sol}^2 / \text{eV}^2 < 1.9 \times 10^{-4}$ and $0.29 < \tan^2 \theta_3 < 0.82$. These (3σ CL) ranges arise from the global statistical analysis [6] of many experimental data coming from neutrino fluxes of accelerator (K2K [7]), reactor (CHOOZ, KAMLAND,... [8,9]), atmospheric (SK,

MACRO, SOUDAN-2 [10]–[12]) and solar (Kamiokande, SK, SNO,...[13]–[19]) origin. The smallness of θ_2 and the hierarchy of mass splittings implies that the oscillations of atmospheric and solar neutrinos are dominantly two-flavour oscillations, described by a single mixing angle and mass splitting: $\theta_{atm} \equiv \theta_1$, $\Delta m_{atm}^2 \equiv \Delta m_{31}^2 \sim \Delta m_{32}^2$ and $\theta_{sol} \equiv \theta_3$, $\Delta m_{sol}^2 \equiv \Delta m_{21}^2$.

Concerning the overall scale of neutrino masses, the non-observation of neutrinoless double β -decay requires the ee element of \mathcal{M}_ν to satisfy [20]

$$\mathcal{M}_{ee} \equiv |m_1 c_2^2 c_3^2 + m_2 c_2^2 s_3^2 + m_3 s_2^2| \lesssim 0.27 \text{ eV} . \quad (4)$$

In addition, Tritium β -decay experiments [21], set the bound $m_i < 2.2$ eV for any mass eigenstate with a significant ν_e component. Finally, astrophysical observations of great cosmological importance, like those of 2dFGRS [22] and especially WMAP [23] set the limit $\sum_i |m_i| < 0.69$ eV. This still allows three possibilities for the neutrino spectrum: hierarchical ($m_1^2 \ll m_2^2 \ll m_3^2$), inverted-hierarchical ($m_1^2 \simeq m_2^2 \gg m_3^2$) and quasi-degenerate ($m_1^2 \simeq m_2^2 \simeq m_3^2$).

The nearly bi-maximal structure of the neutrino mixing matrix, V , is very different from that of the quark sector, where all the mixings are small. An attractive possibility to explain this is that some neutrino mixings are radiatively enhanced, i.e. are initially small and get large in the Renormalization Group (RG) running from high to low energy (RG effects on neutrino parameters have been discussed in [24]–[61]). This amplification effect has been considered at large in the literature [25,30], [51]–[61], but quite often the analyses were incomplete or even incorrect.

In this paper we carefully examine this mechanism for radiative amplification of mixing angles, paying particular attention to 1) a complete treatment of all neutrino parameters (to ensure that not only mixing angles but also mass splittings agree with experiment at low energy) and 2) the fine-tuning price of amplification. We perform this analysis in conventional scenarios, like the Standard Model (SM) or the Minimal Supersymmetric Standard Model (MSSM) and confront them with unconventional supersymmetric scenarios, proposed recently, in which neutrino masses originate in the Kähler potential [46].¹ The sources of neutrino masses in both types of scenarios and their renormalization group equations (RGEs) are reviewed in Section 2, which also

¹We restrict our analysis to the simplest low-energy effective models for neutrino masses, with no other assumptions on the physics at high-energy. We therefore do not discuss RG effects in see-saw scenarios, which have been considered previously, *e.g.* in [28,30,49].

includes a generic discussion of the presence of infrared pseudo-fixed points (IRFP) in the running of the mixing angles. Section 3 is devoted to the radiative amplification of mixing angles in the conventional scenarios (SM and MSSM): we start with an illustrative toy model of only two flavours and later we apply the mechanism first to the amplification of the solar angle, then to the atmospheric angle and finally to the simultaneous amplification of both. Section 4 deals with the amplification of the mixing angles in the unconventional supersymmetric model which looks quite promising due to its peculiar RG features. We collect some conclusions in Section 5. Appendix A contains quite generic renormalization group equations for neutrino masses and mixing angles, while Appendix B presents renormalization group equations for generic non-renormalizable operators in the Kähler potential (like the ones responsible for neutrino masses in the unconventional scenario discussed in this paper).

2 Sources of neutrino masses and RGEs

2.1 Conventional SM and MSSM

In the SM the lowest order operator that generates Majorana neutrino masses is

$$\delta\mathcal{L} = -\frac{1}{4M}\lambda_{\alpha\beta}(H \cdot L_{\alpha})(H \cdot L_{\beta}) + \text{h.c.}, \quad (5)$$

where H is the SM Higgs doublet, L_{α} is the lepton doublet of the α^{th} family, $\lambda_{\alpha\beta}$ is a (symmetric) matrix in flavor space and M is the scale of the new physics that violates lepton number, L. After electroweak symmetry breaking, the neutrino mass matrix is $\mathcal{M}_{\nu} = \lambda v^2/(4M)$, where $v = 246$ GeV (with this definition λ and \mathcal{M}_{ν} obey the same RGE). This scheme can be easily made supersymmetric. The standard SUSY framework has an operator

$$\delta W = -\frac{1}{4M}\lambda_{\alpha\beta}(H_2 \cdot L_{\alpha})(H_2 \cdot L_{\beta}), \quad (6)$$

in the superpotential W , giving $\mathcal{M}_{\nu} = \lambda\langle H_2^0 \rangle^2/(2M) = \lambda v^2 \sin^2 \beta/(4M)$ (with $\tan \beta = \langle H_2^0 \rangle/\langle H_1^0 \rangle$). Both in the SM and the MSSM the energy-scale evolution of \mathcal{M}_{ν} is governed by a RGE [24]–[27] of the form ($t = \log Q$):

$$\frac{d\mathcal{M}_{\nu}}{dt} = -(u_M\mathcal{M}_{\nu} + c_M P_E \mathcal{M}_{\nu} + c_M \mathcal{M}_{\nu} P_E^T), \quad (7)$$

where $P_E \equiv Y_E Y_E^\dagger / (16\pi^2)$ with Y_E the matrix of leptonic Yukawa couplings. The model-dependent quantities u_M and c_M are given in Appendix A. Notice that the non-renormalizable operator of Eq. (5) [Eq. (6) for the SUSY case] is the only L-violating operator in the effective theory, thus its presence in the right-hand side of Eq. (7). The term $u_M \mathcal{M}_\nu$ gives a family-universal scaling of \mathcal{M}_ν which does not affect its texture, while the interesting non family-universal corrections, that can affect the neutrino mixing angles, appear through the matrix P_E .

A very important difference between the SM and the MSSM is the value of the squared tau-Yukawa coupling in P_E . One has:

$$y_\tau^2 = \begin{cases} \frac{2m_\tau^2}{v^2}, & \text{(SM)} \\ \frac{2m_\tau^2}{v^2 \cos^2 \beta} = \frac{2m_\tau^2}{v^2} (1 + \tan^2 \beta). & \text{(MSSM)} \end{cases} \quad (8)$$

Therefore, RG effects can be much larger in the MSSM for sizeable $\tan \beta$.

2.2 Neutrino masses from the Kähler potential

Operators that violate L-number in the Kähler potential, K , offer an alternative supersymmetric source of neutrino masses [46]. The lowest-dimension (non-renormalizable) operators of this kind (that respect R -parity) are

$$\delta K = \frac{1}{2M^2} \kappa_{\alpha\beta} (L_\alpha \cdot H_2) (L_\beta \cdot \bar{H}_1) + \frac{1}{4M^2} \kappa'_{\alpha\beta} (L_\alpha \cdot \bar{H}_1) (L_\beta \cdot \bar{H}_1) + \text{h.c.}, \quad (9)$$

where κ , κ' are dimensionless matrices in flavour space and $\bar{H}_1 = -i\sigma_2 H_1^*$. While κ' is a symmetric matrix, κ may contain a symmetric and an antisymmetric part: $\kappa \equiv \kappa_S + \kappa_A$. These operators give a neutrino mass matrix [46]

$$\mathcal{M}_\nu = \frac{\mu v^2}{M^2} \left[\kappa_S \sin^2 \beta + \kappa' \sin \beta \cos \beta \right], \quad (10)$$

where μ is the SUSY Higgs mass in the superpotential, $W \supset \mu H_1 \cdot H_2$. If W also contains the conventional operator (6), the contribution (10) is negligible in comparison (by a factor $\mu/M \ll 1$). As shown in [46] there are symmetries that can forbid the operator (6) and leave (10) as the only source of neutrino masses. This is our assumption for this scenario. Moreover, as we discuss below, interesting new effects appear through the matrix κ . Therefore we focus on it as the main source of neutrino masses and set

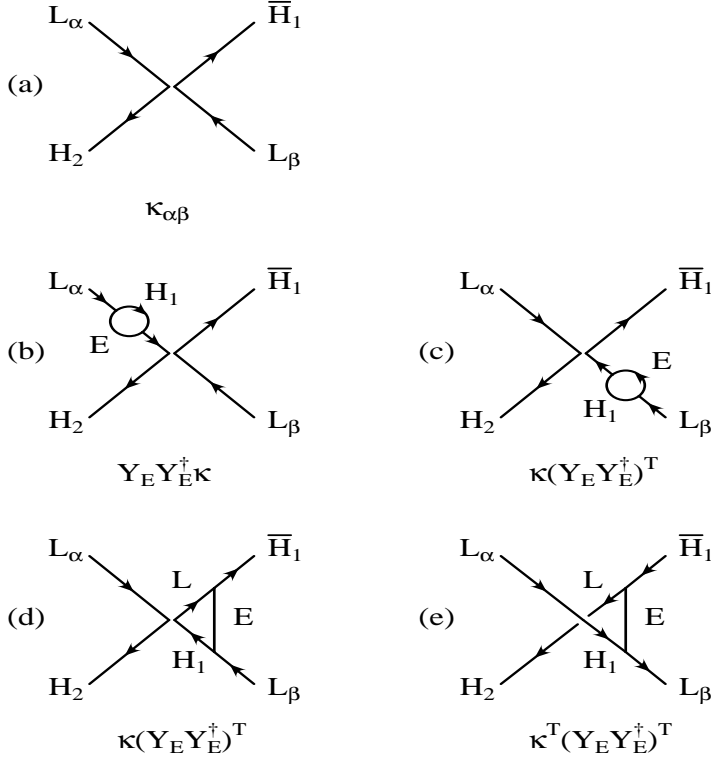


Figure 1: The coupling $\kappa_{\alpha\beta}$ and one-loop texture-changing radiative corrections to it. The lines labelled E represent right-handed (charged) lepton superfields.

$\kappa' = 0$. This can also be the result of some symmetry [46] or be a good approximation if the mass that suppresses the κ' operator is much larger than that for κ . Another possibility is that $\tan\beta$ is large (as is common in this context), in which case the contribution of κ' to neutrino masses is suppressed by $\sim 1/\tan\beta$. Finally, note that, due to the extra suppression factor μ/M , in this scenario M is much smaller than in the conventional case.

Appendix B presents the RGEs for some non-renormalizable couplings in the Kähler potential, of which κ and κ' are particular examples. The matrix κ' obeys a RGE of the form (7) and therefore behaves like the conventional case, while the RGE for κ has a remarkable structure [46]

$$\frac{d\kappa}{dt} = u\kappa + P_E\kappa - \kappa P_E^T + 2(P_E\kappa - \kappa^T P_E^T), \quad (11)$$

where $16\pi^2 u = \text{Tr}(3Y_U^\dagger Y_U + 3Y_D^\dagger Y_D + Y_E^\dagger Y_E) - 3g_2^2 - g_1^2$. Here $Y_{U(D)}$ is the matrix of up (down) quark Yukawa couplings while g_2 and g_1 are the $SU(2)_L$ and $U(1)_Y$ gauge couplings, respectively.

Besides the usual universal piece, $u\kappa$, there are two different terms that can change

the texture of κ and are therefore the most interesting. The first, $P_E\kappa - \kappa P_E^T$, decomposes in a symmetric and an antisymmetric part. In that order:

$$P_E\kappa - \kappa P_E^T = (P_E\kappa_A - \kappa_A P_E^T) + (P_E\kappa_S - \kappa_S P_E^T) . \quad (12)$$

The second texture-changing term, $2(P_E\kappa - \kappa^T P_E^T)$, is antisymmetric and, therefore, contributes only to the RG evolution of κ_A , the antisymmetric part of κ .

The diagrammatic origin of these contributions is explained with the help of figure 1. Diagram (a) is a tree-level supergraph for the coupling $\kappa_{\alpha\beta}$. The order of subindices is important: L_α is $SU(2)$ -contracted with H_2 ; L_β with \overline{H}_1 . This is depicted in figure 1 by the two "branches" of the vertex, with arrows indicating the order in the $SU(2)$ product. We do not show the one-loop supergraphs that contribute to the universal renormalization of $\kappa_{\alpha\beta}$ but focus on those that can change its texture. Diagrams (b) and (c) renormalize $\kappa_{\alpha\beta}$ through the anomalous dimensions of the leptonic legs, L_α, L_β . These kinds of diagrams are proportional to $P_E\kappa$ and κP_E^T , as indicated, and are also present when neutrino mass operators arise from the superpotential. They contribute a $P_E\kappa + \kappa P_E^T$ piece to the renormalization of κ . Diagrams (d) and (e) are non zero only because κ involves chiral and anti-chiral fields. Similar vertex corrections are absent for the neutrino mass operator in W , which involves only chiral fields, and is protected by SUSY non-renormalization theorems. Diagram (d) gives a contribution similar to that coming from diagram (c) but twice as large and with opposite sign. The net effect is to change $P_E\kappa + \kappa P_E^T$ [from (b)+(c)] into $P_E\kappa - \kappa P_E^T$. This is the origin of the first term in the RGE (11). Finally, diagram (e) gives only a correction to the operator $(L_\alpha \cdot L_\beta)(\overline{H}_1 \cdot H_2)$, which is the antisymmetric part of $\kappa_{\alpha\beta}$ by virtue of the identity $r_{\alpha\beta}(L_\alpha \cdot L_\beta)(\overline{H}_1 \cdot H_2) = (r_{\beta\alpha} - r_{\alpha\beta})(L_\alpha \cdot H_2)(L_\beta \cdot \overline{H}_1)$ and this is responsible for the last term $2(P_E\kappa - \kappa^T P_E^T)$ in (11).

In order to show more clearly the structure of the RGE for κ , Eq. (11), it is convenient to split it in two: one for the symmetric part, κ_S , that is directly responsible for neutrino masses, and another for the antisymmetric part, κ_A , that does not contribute to neutrino masses. One gets

$$\frac{d\kappa_S}{dt} = u\kappa_S + P_E\kappa_A - \kappa_A P_E^T , \quad (13)$$

$$\frac{d\kappa_A}{dt} = u\kappa_A + P_E\kappa_S - \kappa_S P_E^T + 2(P_E\kappa - \kappa^T P_E^T) . \quad (14)$$

As explained in [46], the RGE for κ_S has the remarkable property of being dependent of

κ_S itself only through the universal piece. We have shown in more detail here how this arises from a cancellation involving corrections that are only present in supersymmetry for couplings in the Kähler potential. Non-supersymmetric two-Higgs-doublet models also have vertex corrections, but there is no such cancellation there. Some interesting implications that follow from the RGEs (13, 14) were presented in [46].² In this paper we will study in detail the possibilities they offer for amplifying neutrino mixing angles in a natural way.

2.3 Infrared pseudo-fixed points (IRFP) for mixing angles

Equations (7) and (13) detail how \mathcal{M}_ν receives a non-universal RG perturbation which is in general modest (P_E is dominated by y_τ^2 , which is very small, unless $\tan\beta \gtrsim 50$). However, when \mathcal{M}_ν has (quasi-)degenerate eigenvalues ($m_i \simeq m_j$), even small perturbations can cause large effects in the eigenvectors (*i.e.* in the form of V). This can be easily understood: for exact degeneracy there is an ambiguity in the choice of the associated eigenvectors, and thus in the definition of V . When the perturbation due to RG running is added, the degeneracy is lifted and a particular form of V is singled out. If the initial degeneracy is not exact, the change of V will be large or not depending on the size of the perturbation ($\delta_{RG}\Delta m_{ij}^2$) compared with the initial mass splitting at the scale M , $\Delta m_{ij}^2(M)$.

When the RG effect dominates, V evolves quickly from its initial value $V^{(0)}$ to a stable form (an infrared pseudo-fixed point, IRFP) $V^{(0)}R_{ij}$ where R_{ij} is a rotation in the plane of the two quasi-degenerate states i, j such that the perturbation of \mathcal{M}_ν is diagonal in the rotated basis (as is familiar from degenerate perturbation theory). Scenarios in which this takes place are attractive for two main reasons: 1) some particular mixing angle will be selected as a result of V approaching its IRFP form and 2) the i - j mass-splitting will be essentially determined at low energy by RG effects.

When $\delta_{RG}\Delta m_{ij}^2 \sim \Delta m_{ij}^2(M)$, RG effects can produce substantial changes in V without getting too close to the IRFP. This scenario is of interest because, as we show in Sect. 3, the IRFP form of V in the SM and the MSSM is not in agreement with experimental observations, while intermediate forms of V can be.

²For instance, if initially $\kappa_S = 0$ the whole neutrino mass matrix is generated as a radiative effect through (13). Such matrix has precisely the texture of the Zee model [62] (actually, this possibility can be understood as the supersymmetrization of the Zee model).

3 Amplification of mixing angles: SM and MSSM

As explained above, when two neutrino masses are quasi-degenerate (and with the same sign) radiative corrections can have a large effect on neutrino mixing angles. This offers an interesting opportunity for generating large mixing angles at low energy as an effect of RG evolution, starting with a mixing angle that might be small. This possibility has received a great deal of attention in the literature [25,30], [51]–[61]. Here we explain why the implementation of this idea in the SM or the MSSM is not as appealing as usually believed. In order to show this we will make much use of the RGEs for physical parameters derived in Ref. [30] and collected in Appendix A for convenience.

Radiative corrections to V are very small unless $|\epsilon_\tau \nabla_{ij} \log(M/M_Z)| \gtrsim 1$ for some i, j [see Eqs. (A.3, A.15); here $\epsilon_\tau \sim y_\tau^2/(16\pi^2)$ and ∇_{ij} was defined in the Introduction] which generically requires mass degeneracy, both in absolute value and sign (i.e. $m_i \simeq m_j \Rightarrow |\nabla_{ij}| \gg 1$), except for the SUSY case with very large $\tan\beta$, and thus large ϵ_τ .³ In general, if $m_i \simeq m_j$, so that $|\nabla_{ij}|$ dominates the RGEs of $V_{\tau i}$, $V_{\tau j}$, these quantities change appreciably, but the following quantities will be approximately constant

$$\left. \begin{array}{l} \Delta_{ij} V_{\tau i} V_{\tau j} , \\ V_{\alpha l} , (l \neq i, j) \end{array} \right\} \simeq \text{RG - invariant} , \quad (15)$$

where $\Delta_{ij} = 1/\nabla_{ij}$. The IRFP form for V can be deduced from Eq. (A.3) and corresponds to $T_{ij} = 0$, which for sizeable $\epsilon_\tau \nabla_{ij}$ implies $V_{\tau i} = 0$ or $V_{\tau j} = 0$ (depending on the sign of ∇_{ij}). Such V can not give the observed angles (it could if the SAMS solution were still alive).

Hence, the IRFP form for V should *not* be reached. Still, one may hope that the RG effects could amplify the atmospheric and/or the solar angles without reaching the IRFP form of V . Such possibility would be acceptable only if 1) all mixing angles and mass splittings (which are also affected by the running) agree with experiment and 2) if this can be achieved with no fine-tuning of the initial conditions.

We explore in turn the possibility of RG amplification of the mixing angle in a two-flavour case and then for the solar or/and atmospheric angles.

³If $|\epsilon_\tau \log(M/M_Z)| \sim \mathcal{O}(1)$ the validity of the one-loop approximation is in doubt and the analysis of RG evolution should be done by numerical integration of the RGEs in order to capture the leading-log effects at all loops.

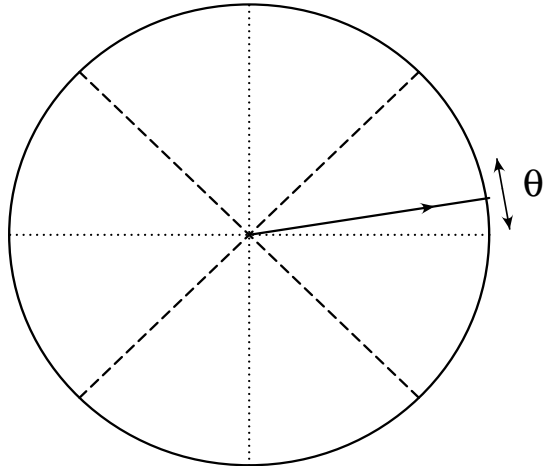


Figure 2: Pictorial representation of the pseudo-fixed points of the mixing angle θ : 0 and $\pi/2$ in dotted lines, $\pm\pi/4$ in dashed lines. The initial condition for θ is represented by a solid line and the two arrows represent the two possible evolutions of the running angle.

3.1 The two-flavour approximation

There are several instances (see below) in which the evolution of a particular mixing angle is well approximated by a two-flavour model. This simple setting is very useful to understand the main features of the RG evolution of mixings and mass splittings, and thus the form of the infrared fixed points and the potential fine-tuning problems associated with mixing amplification.

In a two-flavour context we have flavour eigenstates, (ν_α, ν_β) , a mixing angle, θ , (with $V_{\alpha 2} \equiv \sin \theta$ and $\nu_\alpha = \nu_1$ for $\theta = 0$) and mass eigenstates (eigenvalues), ν_i (m_i), $i = 1, 2$. In a basis where the matrix of leptonic Yukawa couplings is diagonal, the RGE for the mixing angle [from Eq. (A.3)] takes the form

$$\frac{d\theta}{dt} = -\frac{1}{2}\epsilon_{\alpha\beta}\nabla_{21}\sin 2\theta . \quad (16)$$

with

$$\epsilon_{\alpha\beta} \equiv c_M \frac{y_\alpha^2 - y_\beta^2}{16\pi^2} , \quad (17)$$

where c_M is a model-dependent constant. As previously discussed, for $|\nabla_{21}| \gg 1$ (i.e. for quasi-degenerate neutrinos), θ can change appreciably. In such case, it will be driven towards the infrared (pseudo)-fixed point θ^* determined by the condition $d\theta/dt = 0$, which corresponds to $\theta^* = 0, \pi/2$, that is, towards zero mixing, $\sin 2\theta^* = 0$. The degree of approximation to this fixed point depends on the length of the running interval, $[\log(M/M_Z)]$, on the values of the Yukawa couplings, and especially on ∇_{21} . On the

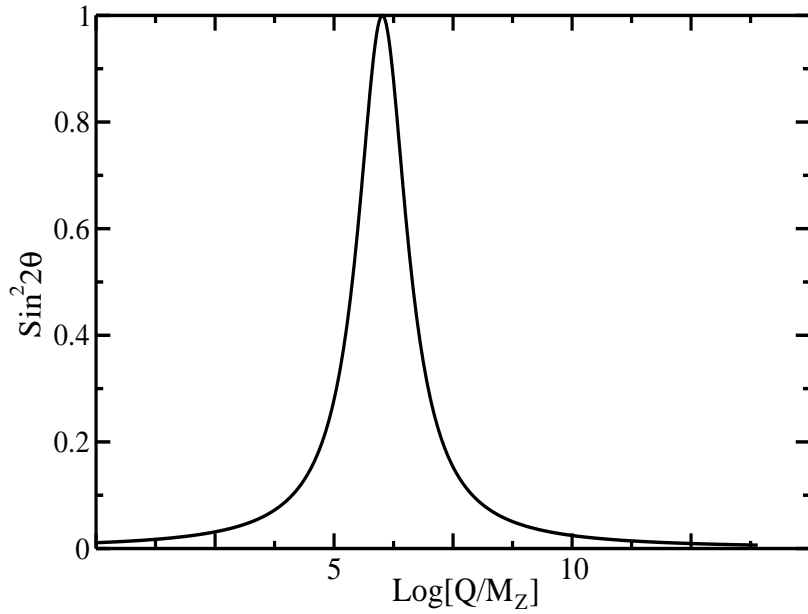
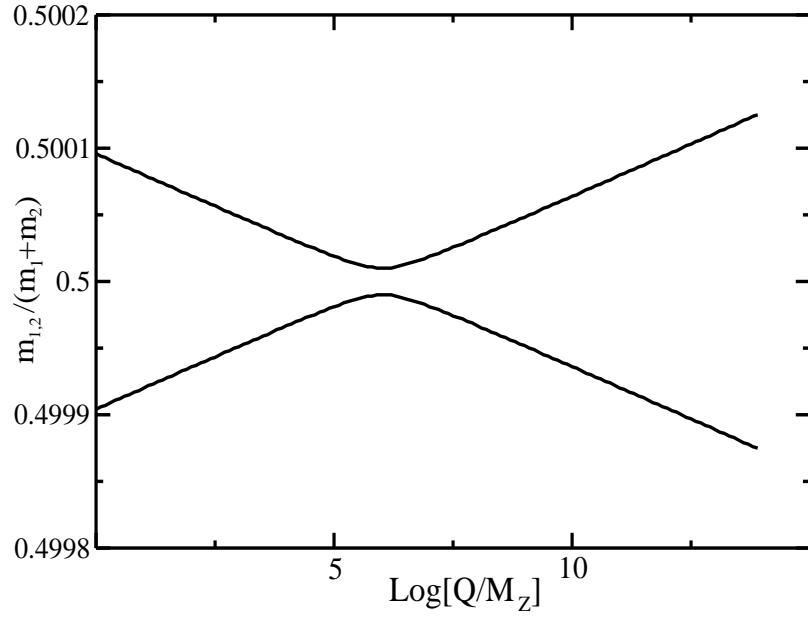


Figure 3: Running of $m_1/(m_1 + m_2)$ and $m_2/(m_1 + m_2)$ (upper plot) and $\sin^2 2\theta$ (lower plot) from M down to M_Z in a two-flavour model with quasi-degenerate masses.

other hand the relative splitting, Δ_{21} satisfies the RGE [from Eq. (A.11)]

$$\frac{d\Delta_{21}}{dt} = \frac{4m_1m_2}{(m_1+m_2)^2} \epsilon_{\alpha\beta} \cos 2\theta \simeq \epsilon_{\alpha\beta} \cos 2\theta , \quad (18)$$

where, for the last approximation, we have assumed quasi-degenerate neutrinos, which is the case of interest. As a consequence, note that

$$\Delta_{21} \sin 2\theta \simeq \text{RG} - \text{invariant} . \quad (19)$$

There are two qualitatively different possibilities for the running of θ depending on the sign of $d\theta/dt$ at M (see figure 2, where the fixed points for θ are indicated by dotted lines): if θ decreases with decreasing scale ($d\theta/dt > 0$ at M) and $\theta^{(0)} \equiv \theta(M)$ is small, the RG evolution drives θ to zero in the infrared, making it even smaller: the mixing never gets amplified. On the opposite case, if θ increases with decreasing scale ($d\theta/dt < 0$ at M), θ is driven towards $\theta^* = \pi/2$, and it may happen that the running stops (at M_Z) near $\theta \sim \pi/4$ so that large mixing is obtained.⁴ In this second case the RG-evolution is illustrated by figure 3. The upper plot shows the running of $m_1/(m_1+m_2)$ and $m_2/(m_1+m_2)$ with the scale (this choice removes the universal part of the running and focuses on the interesting relative mass splitting) while the lower plot shows the running of $\sin^2 2\theta$. Notice that the evolution of the splitting is quite smooth (first decreasing and then increasing), while the change of θ is only important around the scale of maximal mixing ($\theta \sim \pi/4$) which corresponds to the scale of minimal splitting. A simple analytical understanding of this behaviour is possible in the case of interest, with quasi-degenerate masses. In that case the RGEs for θ and Δ_{21} , Eqs. (16, 18), can be integrated exactly (assuming also that the running of y_τ^2 is neglected) to get

$$\sin^2 2\theta(Q) = \frac{[\Delta_{21}^{(0)} \sin 2\theta^{(0)}]^2}{\left[\Delta_{21}^{(0)} \cos 2\theta^{(0)} - \epsilon_{\alpha\beta} \log \frac{M}{Q} \right]^2 + [\Delta_{21}^{(0)} \sin 2\theta^{(0)}]^2} , \quad (20)$$

$$\Delta_{21}^2(Q) = \left[\Delta_{21}^{(0)} \cos 2\theta^{(0)} - \epsilon_{\alpha\beta} \log \frac{M}{Q} \right]^2 + [\Delta_{21}^{(0)} \sin 2\theta^{(0)}]^2 . \quad (21)$$

From these solutions we can immediately obtain the scale Q_{max} at which maximal mixing occurs:

$$\log \frac{M}{Q_{max}} = \frac{\Delta_{21}^{(0)}}{\epsilon_{\alpha\beta}} \cos 2\theta^{(0)} ; \quad (22)$$

⁴For the solar angle, one should have $\tan^2 \theta_3(M_Z) < 1$ (with eigenvalues labelled such that $|m_1| < |m_2|$ holds at low energy), as needed for the MSW solution [5].

the half-width, ω , of the 'resonance' (defined at $\sin^2 2\theta = 1/2$)

$$\omega = \frac{\Delta_{21}^{(0)}}{\epsilon_{\alpha\beta}} \sin 2\theta^{(0)} ; \quad (23)$$

and the minimal splitting:

$$\Delta_{21,min} \equiv \Delta_{21}(Q_{max}) = \Delta_{21}^{(0)} \sin 2\theta^{(0)} . \quad (24)$$

These results make clear that amplification requires a fine-tuning of the initial conditions. Suppose one desires that the initially small value of the mixing, $\sin 2\theta^{(0)}$, gets amplified by a factor $F \gg 1$ at low energy due to the running. From (19), this requires the initial relative splitting, $\Delta_{21}^{(0)}$ to be fine-tuned to the RG shift, $\delta_{RG}\Delta_{21}$, as

$$\begin{aligned} \Delta_{21}^{(0)} &= F\Delta_{21}(M_Z) = F[\Delta_{21}^{(0)} + \delta_{RG}\Delta_{21}] \\ \Rightarrow \delta_{RG}\Delta_{21} &= -\left(1 - \frac{1}{F}\right)\Delta_{21}^{(0)} , \end{aligned} \quad (25)$$

where⁵

$$\delta_{RG}\Delta_{21} \simeq \epsilon_{\alpha\beta} \cos 2\theta \log \frac{M}{M_Z} . \quad (26)$$

Hence, Eq. (25), which makes quantitative the arguments of the last paragraph of Sect. 2.3, exposes a fine-tuning of one part in F between two completely unrelated quantities. There is no (known) reason why these two quantities should be even of a similar order of magnitude, which stresses the artificiality of such coincidence.

Alternatively, this fine-tuning can be seen in the expressions for the scale Q_{max} and the half-width ω [Eqs. (22, 23)]. The initial splitting, $\Delta_{21}^{(0)}$, and the strength of the radiative effect, $\epsilon_{\alpha\beta}$, have to be right to get Q_{max} near M_Z : If $\Delta_{21}^{(0)}$ is small and/or $\epsilon_{\alpha\beta}$ is large, the angle goes through maximal mixing too quickly; if $\Delta_{21}^{(0)}$ is large and/or $\epsilon_{\alpha\beta}$ is small, the angle never grows appreciably. How delicate the balance must be is measured by the half-width ω , or better its ratio to the running interval,

$$\frac{\omega}{\log(M/Q_{max})} = \tan 2\theta^{(0)} , \quad (27)$$

which is of order $1/F$ in agreement with the previous estimate of the fine-tuning. Finally, notice from (25) that the RG-shift must satisfy $\delta_{RG}\Delta_{21} = (1 - F)\Delta_{21}^{exp}$, which may be impossible or unnatural to arrange, as we show in some examples below.

⁵This is a one-loop leading-log approximation valid when $\sin^2 2\theta^{(0)} \ll 1$. A more precise result is given by the exact expression in Eq. (21), which includes all leading-log corrections.

3.2 Solar angle

To amplify only the solar angle, $\theta_{sol} \equiv \theta_3$, the RGE of V must be dominated by ∇_{21} [see (A.19)], which requires a quasi-degenerate ($m_1 \simeq m_2 \simeq |m_3|$) or inversely-hierarchical ($m_1 \simeq m_2 \gg |m_3|$) spectrum. Then the RG-corrected V is $V^{(0)}R_{12}(\phi)$ with ϕ evolving towards an IRFP such that $V_{\tau 1} = 0$ or $V_{\tau 2} = 0$, while $V_{\alpha 3} = (s_2, s_1 c_2, c_1 c_2)^T$ is almost unaffected by the running. This means, in particular, that θ_1 and θ_2 have to be determined by the physics at M , so as to have $V_{\alpha 3} \simeq (0, 1/\sqrt{2}, 1/\sqrt{2})^T$ as an initial condition. An attractive feature of this scenario is that the running would not upset such initial values as only θ_3 is affected. This is most clearly seen by realizing that $V \rightarrow V^{(0)}R_{12}(\phi)$ amounts simply to $\theta_3 \rightarrow \theta_3^{(0)} + \phi$ [see (3)].

It is a good approximation to treat the running of θ_3 in a two-flavour context [see Eqs. (16) and (A.19)] with $(\nu_\alpha, \nu_\beta) \equiv (\nu_e, \nu_\mu \cos \theta_1 - \nu_\tau \sin \theta_1)$, and $(m_i, m_j) = (m_1, m_2)$. Therefore we can apply the results obtained in the previous subsection [in particular Eqs. (16, 18) with $y_\alpha^2 \simeq 0$, $y_\beta^2 \simeq s_1^2 y_\tau^2 \simeq y_\tau^2/2$] to conclude that the amplification of $\sin 2\theta_3$ by a factor $F \gg 1$ requires a fine-tuning of one part in F between two completely unrelated quantities: the relative mass splitting at the M scale, $\Delta_{21}^{(0)}$, and the splitting generated radiatively, $\delta_{RG}\Delta_{21}$.

Moreover, from Eqs. (25, 26), $\delta_{RG}\Delta_{21} \simeq (\epsilon_\tau/2) \log(M/M_Z)$ has to match $(1 - F)\Delta_{21}^{exp}$. In the SM $\delta_{RG}\Delta_{21}$ is quite small, which means that F must be close to one: $F - 1 \simeq 10^{-3} \log(M/M_Z)(7 \times 10^{-5} \text{eV}^2/\Delta m_{sol}^2)(m/0.2 \text{eV})^2$. Consequently, it is not possible to amplify the solar angle in the SM, even with fine-tunings. Larger values of $\delta_{RG}\Delta_{21}$ can be achieved in the MSSM for large $\tan \beta$: amplification of $\sin 2\theta_3$ by a factor F requires

$$\tan \beta \simeq 37 \sqrt{\frac{(F - 1)}{\log(M/M_Z)} \left(\frac{\Delta m_{sol}^2}{7 \times 10^{-5} \text{eV}^2} \right)^{1/2} \left(\frac{0.2 \text{eV}}{m} \right)}, \quad (28)$$

where $\log(M/M_Z) \sim 30$ is a typical value.

3.3 Atmospheric angle

This case was critically examined already in [30,55]. We summarize here the main arguments and results and complete the analysis. From Eqs. (A.17–A.19), the amplification of $\theta_{atm} \equiv \theta_1$ requires that ∇_{31} or ∇_{32} dominate the RGEs, and therefore

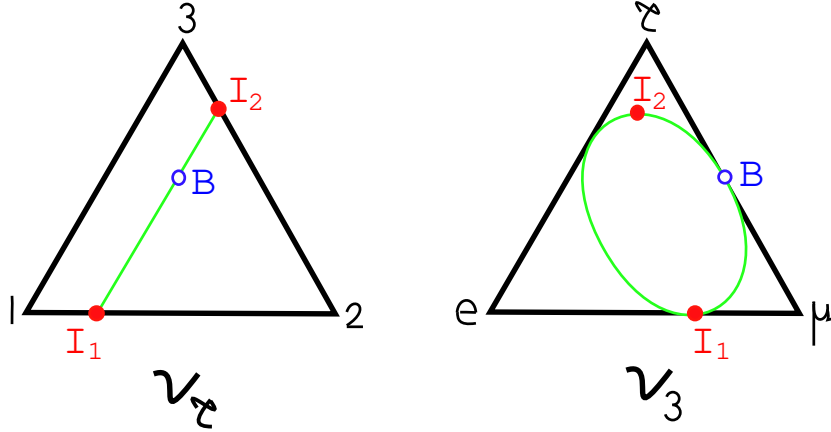


Figure 4: RG trajectory of V in matrix space for $|\nabla_{32}| \gg 1$. The red solid dots represent IRFPs, while the blue empty dots represent the bi-maximal mixing point for the atmospheric and solar angles.

$m_1 \simeq -m_2 \simeq \pm m_3$ is necessary.⁶

Suppose that ∇_{31} is dominant (for ∇_{32} the argument is similar). The RG-corrected mixing matrix takes the form $V = V^{(0)}R_{31}(\phi)$, with ϕ evolving towards an IRFP such that $V_{\tau 1} = 0$ or $V_{\tau 3} = 0$ while $V_{\alpha 2}$ remains almost constant.⁷ Therefore, to agree with experiment we must assume as an initial condition $V_{\alpha 2} \simeq (1/\sqrt{2}, 1/2, -1/2)^T$. As ϕ changes, the path of V in matrix space goes through a bi-maximal mixing form. This (closed) path is represented in figure 4 which makes use of triangular diagrams [63] to represent V by a pair of points inside two equilateral triangles of unit height. A point inside the left triangle (say B) determines three distances to each side, which correspond to $|V_{\tau 1}|^2$, $|V_{\tau 2}|^2$ and $|V_{\tau 3}|^2$ (with the unitary condition $\sum_i |V_{\tau i}|^2 = 1$ ensured geometrically). On the right triangle the point B determines instead $|V_{e 3}|^2$, $|V_{\mu 3}|^2$ and $|V_{\tau 3}|^2$ (redundance in the latter requires the points to be drawn with the same height on both sides).

In figure 4 the green path is traversed as ϕ is varied, with IRFPs marked by solid red dots (I_1 , I_2). By assumption we start the running at some point in this path near $\sin^2 2\theta_1 = 0$, *i.e.* near the intersections with the $e\tau$ -side ($\theta_1 = 0$) or the $e\mu$ -side ($\theta_1 = \pi/2$). Maximal θ_1 mixing corresponds to points equidistant from these two sides. The goal would be to stop the running near the point B marked by the open blue dot, which has maximal θ_1 mixing and zero θ_2 . From the location of the IRFP points, this

⁶Another possibility, with $m_1 \simeq m_2 \simeq m_3$, is discussed in Sect. 3.4.

⁷The two-flavour approximation is not possible here: it requires $s_2 \simeq s_3 \simeq 0$, at odds with experiment.

amplification can only work if we start near $\theta_1 = \pi/2$ (starting near $\theta_1 = 0$ we can never reach our goal) and have $|V_{e3}|^2 < 1/3$ (so as to take the right path). Schematically, this right path from one IRFP to the other going through the point of bi-maximal mixing is

$$V_{I_1} \equiv \begin{pmatrix} \frac{1}{\sqrt{6}} & \frac{1}{\sqrt{2}} & -\frac{1}{\sqrt{3}} \\ \frac{1}{2\sqrt{3}} & \frac{1}{2} & \frac{2}{\sqrt{6}} \\ \frac{\sqrt{3}}{2} & -\frac{1}{2} & 0 \end{pmatrix} \rightarrow V_B \equiv \begin{pmatrix} \frac{1}{\sqrt{2}} & \frac{1}{\sqrt{2}} & 0 \\ -\frac{1}{2} & \frac{1}{2} & \frac{1}{\sqrt{2}} \\ \frac{1}{2} & -\frac{1}{2} & \frac{1}{\sqrt{2}} \end{pmatrix} \rightarrow V_{I_2} \equiv \begin{pmatrix} -\frac{1}{\sqrt{3}} & \frac{1}{\sqrt{2}} & \frac{1}{\sqrt{6}} \\ \frac{2}{\sqrt{6}} & \frac{1}{2} & \frac{1}{2\sqrt{3}} \\ 0 & -\frac{1}{2} & \frac{\sqrt{3}}{2} \end{pmatrix}$$

(a change in the sign of ∇_{31} reverses the direction of the arrows). Under these assumptions amplification at the right scale still requires a certain fine-tuning, similar to the one discussed in the previous section.

In addition there is now an even worse drawback because it is difficult to do this tuning without upsetting Δm_{sol}^2 : the relative mass splittings are approximately given by [from (A.11)]

$$\frac{\Delta m_{atm}^2}{m^2} = \left[\frac{\Delta m_{31}^2}{m^2} \right]^{(0)} + 4\epsilon_\tau \langle V_{\tau 3}^2 - V_{\tau 1}^2 \rangle \log \frac{M}{M_Z}, \quad (29)$$

$$\frac{\Delta m_{sol}^2}{m^2} = \left[\frac{\Delta m_{21}^2}{m^2} \right]^{(0)} + 4\epsilon_\tau \langle V_{\tau 2}^2 - V_{\tau 1}^2 \rangle \log \frac{M}{M_Z}, \quad (30)$$

where $\langle \rangle$ denote averages over the interval of running and m is the overall neutrino mass. We see that both radiative corrections are of similar magnitude because, for rapidly changing $V_{\tau 1}$ and $V_{\tau 3}$, the averages of matrix elements in (29, 30) cannot be suppressed and are therefore of $\mathcal{O}(1)$. On the other hand, $\delta_{RG}(\Delta m_{31}^2/m^2)$ [last term in Eq. (29)] must be $(F - 1)\Delta m_{atm}^2/m^2$, where F is defined as $V_{\tau 1}V_{\tau 3} = FV_{\tau 1}^{(0)}V_{\tau 3}^{(0)}$ [see Eq. (15)]. For a sizeable amplification, $(F - 1) \gtrsim 1$, so unless there is an extremely accurate and artificial cancellation in (30), one naturally expects $\Delta m_{sol}^2 \sim \Delta m_{atm}^2$, which is not acceptable. In fact, there are further problems: in the SM $\delta_{RG}(\Delta m_{31}^2/m^2)$ is not large enough to match $(F - 1)\Delta m_{atm}^2/m^2$. In the MSSM this is possible, but it requires, besides a certain tuning, a very large $\tan \beta$ ($\gtrsim 100$ for $|m| < 0.3$ eV).

3.4 Solar and atmospheric angles simultaneously

There is still a possibility for mixing amplification not discussed in the previous subsections (3.2 and 3.3), namely when $m_1 \simeq m_2 \simeq m_3$, both in absolute value and sign⁸.

⁸This possibility has been recently used in [61], where the implicit fine-tuning we are about to show was not addressed.

Then $\nabla_{21} \gg \nabla_{31} \simeq \nabla_{32} \gg 1$ (in absolute value). Notice from Eq. (A.17–A.19) that if $\epsilon_\tau \nabla_{31} \log(M/M_Z) \sim \mathcal{O}(1)$, so that the atmospheric angle can run appreciably, then it is mandatory that $V_{\tau 1} V_{\tau 2} \simeq 0$; otherwise the running of V will be strongly dominated by the term proportional to $T_{21} = \epsilon_\tau V_{\tau 1} V_{\tau 2} \nabla_{21}$, and thus rapidly driven to an IRFP (a phenomenological disaster). To avoid this, the condition $V_{\tau 1} V_{\tau 2} \simeq 0$ must be fulfilled initially and along most of the running.⁹ In addition one has to demand $V_{\tau 2}^2 - V_{\tau 1}^2 \simeq 0$ along most of the running, otherwise Δm_{21}^2 gets radiative corrections of a size similar to Δm_{atm}^2 for the reasons explained in Subsect. 3.3. In consequence the possibility under consideration can only work if $V_{\tau 2} \simeq V_{\tau 1} \simeq 0 \Rightarrow \sin \theta_1 \simeq \sin \theta_2 \simeq 0$ along most of the running.

The previous conclusion implies that θ_1 must be radiatively amplified at low energy. Actually, it can be checked from Eq. (A.17) that, since $\nabla_{31} \simeq \nabla_{32}$, the running of θ_1 is well approximated by a two-flavour equation (see Subsect. 3.1)

$$\frac{d\theta_1}{dt} \simeq \frac{1}{2} \epsilon_\tau \nabla_{31} \sin 2\theta_1 . \quad (31)$$

Hence, the results of Subsect. 3.1 apply here and we conclude that the amplification of θ_1 requires 1) a very large $\tan \beta$ ($\gtrsim 100$ for $|m| < 0.3$ eV) to get a large enough $\delta_{RG} \Delta_{31}$ and 2) a fine-tuning between the initial splitting $\Delta_{31}^{(0)}$ and the radiative correction $\delta_{RG} \Delta_{31}$:

$$\delta_{RG} \Delta_{31} = - \left(1 - \frac{1}{F} \right) \Delta_{31}^{(0)} . \quad (32)$$

This tuning can also be seen by equations similar to (22) and (23) which in this particular case read

$$\log \frac{M}{M_Z} \simeq \frac{\Delta_{31}^{(0)}}{\epsilon_\tau} \cos 2\theta_1^{(0)} , \quad \omega_1 \simeq \frac{\Delta_{31}^{(0)}}{\epsilon_\tau} \sin 2\theta_1^{(0)} . \quad (33)$$

Besides this, another problem affects the running of θ_3 . The RGE of θ_3 is given by [see Eq. (A.19)]

$$\frac{d\theta_3}{dt} \simeq \frac{1}{2} (\epsilon_\tau \sin^2 \theta_1) \nabla_{21} \sin 2\theta_3 , \quad (34)$$

which is very similar to a two-flavour RGE except for the extra factor $\sin^2 \theta_1$. Clearly, $\sin 2\theta_3$ must be initially small. Otherwise, since $|\nabla_{21}| \gg |\nabla_{31}|$, for moderate values

⁹This condition implies that one starts near one of the IRFPs. To avoid falling towards it, the signs of the splittings must be such that V is eventually driven towards a different IRFP, crossing in its way regions of parameter space with sizeable $V_{\tau 1}$ and $V_{\tau 2}$. [This is similar to the situation discussed after Eq. (19)]

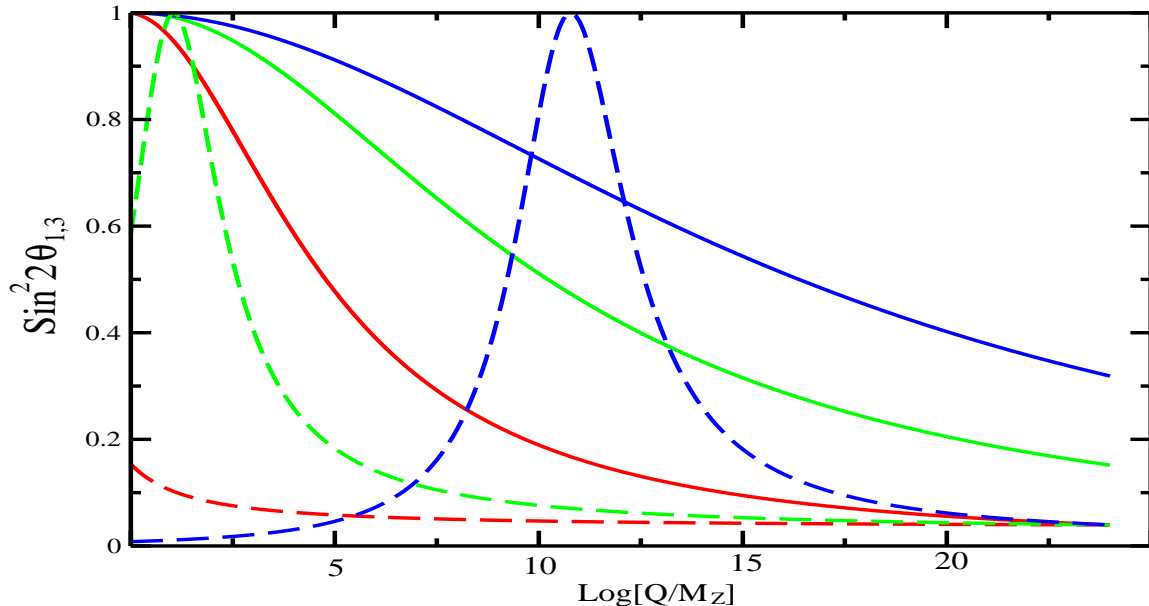


Figure 5: Running of $\sin^2 2\theta_1$ (solid lines) and $\sin^2 2\theta_3$ (dashed lines) from M down to M_Z for different initial values of $\sin^2 2\theta_1$.

of $\sin^2 \theta_1$, θ_3 runs much more quickly than θ_1 and therefore it is driven to the IRFP (with small $\sin 2\theta_3$) before θ_1 gets properly amplified. Consequently, θ_3 needs radiative amplification and this requires its own fine-tuning:

$$\log \frac{M}{Q_{3,max}} \simeq \frac{\Delta_{21}^{(0)}}{\epsilon_\tau \sin^2 \theta_1^{(0)}} \cos 2\theta_3^{(0)}, \quad \omega_3 \simeq \frac{\Delta_{21}^{(0)}}{\epsilon_\tau \sin^2 \theta_1(Q_{3,max})} \sin 2\theta_3^{(0)}. \quad (35)$$

Notice that for estimating the position of the peak in the running of $\sin^2 2\theta_3$ we have simply used the initial value of $\sin^2 \theta_1$ as if it would not run, while for estimating the half-width, ω_3 , a better choice is to use $\sin^2 \theta_1$ at the peak $Q_{3,max}$, which is assumed to be around M_Z . This means in particular that ω_3 is not enlarged significantly by the initial smallness of $\sin^2 \theta_1$ and, being controlled by $\Delta_{21}^{(0)}$, it is in general even smaller than ω_1 . This behaviour is shown in figure 5 where the solid lines give $\sin^2 2\theta_1$ and the dashed ones $\sin^2 2\theta_3$. The three different pairs of curves correspond to different initial conditions for $\sin^2 2\theta_1$, with the $\Delta_{31}^{(0)}$ mass splitting chosen so as to get maximal atmospheric mixing at M_Z . As expected from Eq. (35), when $\sin^2 2\theta_1^{(0)}$ decreases, the narrow peak in $\sin^2 2\theta_3$ moves rapidly to lower scales, making clear the need for an extra fine-tuning to ensure a large solar mixing angle at M_Z .

4 Amplification of mixing angles: Kähler masses

Let us consider now the possibility of radiative amplification of mixing angles in the scenarios described in Section 2.2, *i.e.* when neutrino masses in a supersymmetric model originate from non-renormalizable operators in the Kähler potential [46]. More precisely, we consider only the operator $\kappa(L \cdot H_2)(L \cdot \overline{H}_1)$ as discussed in Sect. 2.2. Then the RG-evolution of mixing angles is described by an equation of the usual form:

$$\frac{dV}{dt} = VT, \quad (36)$$

with the matrix T given by (see Appendix A):

$$T_{ij} = \frac{-1}{16\pi^2} (y_\alpha^2 - y_\beta^2) \frac{V_{\alpha i} V_{\beta j}}{m_i - m_j} m_{\alpha\beta}^A, \quad (37)$$

for $i \neq j$ and $T_{ii} = 0$. Here $m_{\alpha\beta}^A \equiv (M_\nu^A)_{\alpha\beta}$, where the matrix M_ν^A is related to the Kähler matrix κ_A by $M_\nu^A \equiv \mu \kappa_A v^2 / M^2$. The neutrino mass eigenvalues run according to (no sum in i)

$$\frac{dm_i}{dt} = um_i + \frac{y_\alpha^2}{8\pi^2} V_{\alpha i} m_{\alpha\beta}^A V_{\beta i}. \quad (38)$$

The generic condition required to have a significant change in the mixing angles is to have some sizeable T_{ij} , *i.e.*

$$\frac{y_\tau^2}{16\pi^2} \frac{m_{\alpha\tau}^A}{m_i - m_j} \log \frac{M}{M_Z} \gtrsim \mathcal{O}(1). \quad (39)$$

This is consistent with the general arguments of Subsect. 2.3: notice from (38) that the relative splitting, Δ_{ij} , typically gets a correction

$$\delta_{RG} \Delta_{ij} \sim \mathcal{O} \left(\frac{y_\tau^2}{16\pi^2} \frac{m_{\alpha\tau}^A}{m_i + m_j} \log \frac{M}{M_Z} \right). \quad (40)$$

Therefore, important effects in the mixing angles, Eq. (39), occur when the RG-induced (relative) splittings are comparable (or larger) than the initial splitting ($\delta_{RG} \Delta_{ij} \simeq \Delta_{ij}$).

Comparing Eqs. (37, 39) with the conventional T_{ij} , Eq (A.15), we see that it is possible to have now large effects even for neutrino spectra without quasi-degenerate masses, provided the magnitude of the entries of M_ν^A is larger than the mass differences $m_i - m_j$. This implies that, in the new scenario, amplification of mixing angles is a more general phenomenon, which can occur also for spectra that cannot accommodate amplification in conventional models, *e.g.* normal hierarchy or inverted hierarchy with $m_1 \simeq -m_2$.

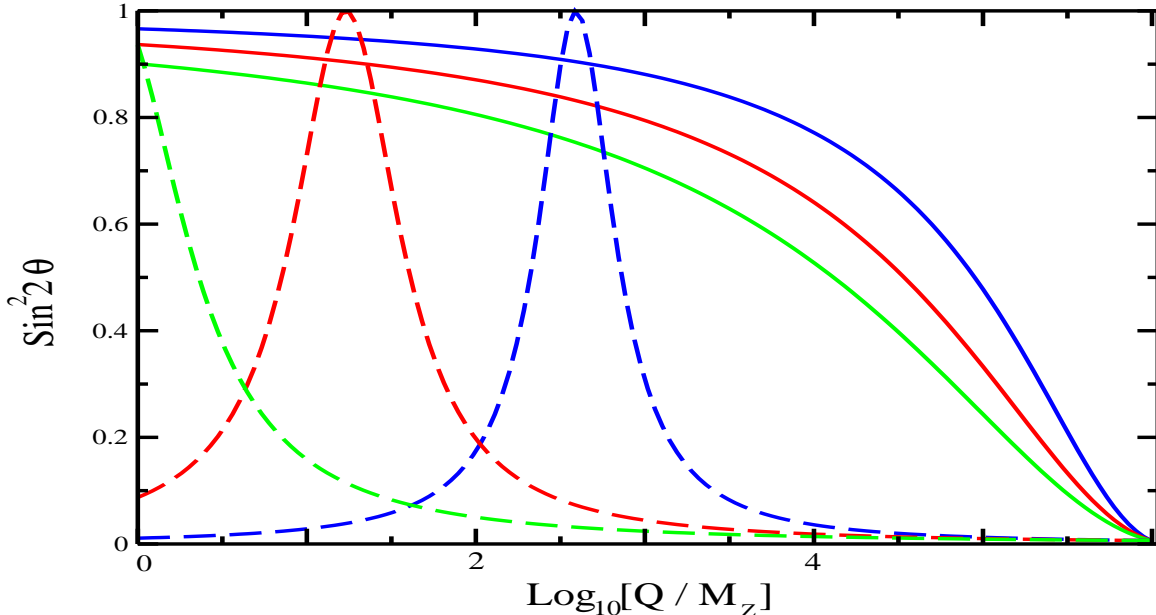


Figure 6: Running of $\sin^2 2\theta$ from M down to M_Z in conventional scenarios (dashed lines) as compared with the Kähler case (solid lines). In each case, different lines correspond to different mass splittings at M .

In parallel with the discussion of the conventional case (Sect. 3) we consider in turn the amplification for a two-flavour case, for the solar angle and for the atmospheric angle.

4.1 Two-flavour scenario

As for the conventional case, the two-flavour model is very useful to understand in a simple setting the main features of the RG evolution of mixings and mass splittings, and the form of the infrared fixed points. In this new scenario the evolution of the mixing angle in a two flavour case does not follow an RGE of the form (16) but rather the following (no sum in α, β):

$$\frac{d\theta}{dt} = -\epsilon_{\alpha\beta} \frac{m_{\alpha\beta}^A}{m_1 - m_2} \cos 2\theta, \quad (41)$$

where again $\epsilon_{\alpha\beta} \equiv (y_\alpha^2 - y_\beta^2)/(16\pi^2)$ with α and β the two flavours and $V_{\alpha 2} \equiv \sin \theta$. Comparing Eq (41) to Eq (16) (i.e. the one for the conventional SM and MSSM cases) we note, beside numerical factors, two main differences: the quantity $\nabla_{12} = (m_1 + m_2)/(m_1 - m_2)$ is replaced by the ratio $m_{\alpha\beta}^A/(m_1 - m_2)$, and $\sin 2\theta$ by $\cos 2\theta$. The first difference implies that important changes on θ are achieved for $|m_{\alpha\beta}^A| \gg |m_1 - m_2|$, which does not require quasi-degeneracy of the eigenvalues. The second one implies

that the running will drive $\cos 2\theta$ (rather than $\sin 2\theta$) to zero, i.e. IRFPs for θ are now at maximal mixing, $\theta^* = \pm\pi/4$ (dashed lines in fig. 2). Therefore, θ will be amplified towards maximal mixing in the infrared¹⁰ irrespective of the sign of $d\theta/dt$ at M and with no fine-tuning required on $m_1 - m_2$.

For comparison with the conventional case, we have plotted in fig. 6 the new evolution of $\sin^2 2\theta(Q)$ in solid lines, for different initial mass splittings; the dashed lines correspond to the running in the conventional scenario (with the same initial conditions). Clearly, in order to generate large neutrino mixing angles through RG evolution, scenarios that follow Eq. (41) are more natural than those that follow Eq. (16). Let us mention that, since M is smaller now, the interval in energy available to amplify θ is also smaller.

Regarding the mass splittings, the quantity $(m_1 - m_2)/m_{\alpha\beta}^A$, which is now the relevant one, satisfies the RGE [from Eqs. (13) and (14)]

$$\begin{aligned} \frac{d}{dt} \left[\frac{m_1 - m_2}{m_{\alpha\beta}^A} \right] &= -2\epsilon_{\alpha\beta} \sin 2\theta \left[1 - \frac{3}{4} \left(\frac{m_1 - m_2}{m_{\alpha\beta}^A} \right)^2 \right] - \frac{1}{8\pi^2} (y_\alpha^2 + y_\beta^2) \frac{m_1 - m_2}{m_{\alpha\beta}^A} \\ &\simeq -2\epsilon_{\alpha\beta} \sin 2\theta , \end{aligned} \quad (42)$$

where, for the last approximation, we have assumed $|m_{\alpha\beta}^A| \gg |m_1 - m_2|$, which is the case of interest. As a consequence, note that

$$\frac{m_1 - m_2}{m_{\alpha\beta}^A} \cos 2\theta \simeq \text{RG - invariant} , \quad (43)$$

in contrast with Eq. (19).

4.2 Solar angle

In the new scenario many of the requirements for amplification of the solar angle are the same as those in conventional cases: the RGE of V should be dominated by T_{21} ; $V_{\alpha 3}$ does not run appreciably and should be fixed as an initial condition to be $\simeq (0, 1/\sqrt{2}, 1/\sqrt{2})^T$ while θ_3 is the only angle that changes significantly. The difference with respect to the standard case is that θ_3 is now driven towards a different IRFP, determined by the condition $T_{21} \rightarrow 0$. In terms of θ_3 and neglecting all leptonic Yukawa

¹⁰Again, for the solar angle, one should have $\tan^2 \theta_3(M_Z) < 1$ (with eigenvalues labelled such that $|m_1| < |m_2|$ holds at low energy), as needed for the MSW solution [5].

couplings other than y_τ this IRFP condition reads

$$\tan 2\theta_3 \rightarrow \frac{2 \sin \theta_2 \cos 2\theta_1 m_{\mu\tau}^A + 2 \sin \theta_1 \cos \theta_2 m_{e\tau}^A}{\sin 2\theta_1 (1 + \sin^2 \theta_2) m_{\mu\tau}^A - \cos \theta_1 \sin 2\theta_2 m_{e\tau}^A} . \quad (44)$$

As this equation clearly shows, the IR behaviour of the running θ_3 does not correspond in general to that expected in a two flavour case (discussed in the previous subsection) but is richer. Several cases of interest are the following:

- If we make the approximation $\sin \theta_2 \simeq 0$, θ_3 evolves towards the IRFP $\tan 2\theta_3^* \simeq m_{e\tau}^A / [\cos \theta_1 m_{\mu\tau}^A]$ and, for $m_{e\tau}^A / m_{\mu\tau}^A \sim \mathcal{O}(1)$ one can easily get θ_3^* inside the experimental range.
- If, in the previous case with $\sin \theta_2 \simeq 0$ one has $m_{e\tau}^A \gg m_{\mu\tau}^A$ (the precise condition is $s_{2\theta_2} \ll m_{\mu\tau}^A / m_{e\tau}^A \ll 1$) the IRFP for θ_3 is at maximal mixing. This case is indeed well described by a two-flavour approximation and can be acceptable if the running interval is not too long so that the low-energy value of θ_3 is not too close to the IRFP.
- If $m_{\mu\tau}^A \simeq 0$ [or, more precisely, $m_{\mu\tau}^A \ll s_{2\theta_2} m_{e\tau}^A$], the IRFP is simply $\tan 2\theta_3^* \simeq -\tan \theta_1 / \sin \theta_2$. That is, this scenario predicts a correlation between the neutrino mixing angles such that, given the experimental interval for θ_3 , the angle θ_2 is predicted to be in the range $0.02 \lesssim \sin^2 \theta_2 \lesssim 0.5$ (for $\tan \theta_1 = 1$). In other words, for θ_3^* in the upper region of its experimentally allowed range, θ_2 lies not far below the CHOOZ bound.

To end the discussion of the solar case one should also check that the requirement of phenomenological low-energy mass splittings is not in conflict with the requirements just described needed to amplify the solar angle. The solar mass splitting, in one-loop leading-log approximation¹¹, is now given by

$$\begin{aligned} \Delta m_{sol}^2 &\simeq \Delta m_{21}^2(M) \left[1 - 2u \log \frac{M}{M_Z} \right] \\ &+ \frac{y_\tau^2}{4\pi^2} \left[(V_{e2} V_{\tau 2} m_2 - V_{e1} V_{\tau 1} m_1) m_{e\tau}^A + (V_{\mu 2} V_{\tau 2} m_2 - V_{\mu 1} V_{\tau 1} m_1) m_{\mu\tau}^A \right] \log \frac{M}{M_Z} . \end{aligned} \quad (45)$$

If the running is long enough to approach the IRFP, in which case the radiative correction of the splitting overcomes the initial value at the M -scale [see the discussion

¹¹Two-loop leading-log corrections $\sim [y_\tau^2 m_{\alpha\tau}^A \log(M/M_Z)/(16\pi^2)]^2$ produce a non-vanishing splitting at low energy even if initially $m_i = 0$. Such corrections can be easily obtained from Eq. (38).

around Eq. (39)], the above result gets simplified to

$$\Delta m_{sol}^2 \simeq (m_1 + m_2)(M_Z) \frac{y_\tau^2}{8\pi^2} \left[(V_{e2}V_{\tau 2} - V_{e1}V_{\tau 1})m_{e\tau}^A + (V_{\mu 2}V_{\tau 2} - V_{\mu 1}V_{\tau 1})m_{\mu\tau}^A \right] \log \frac{M}{M_Z} . \quad (46)$$

The most important aspect of this formula is that, in stark contrast to the standard cases of the SM or the MSSM, the radiative correction to the mass splitting is controlled by the elements of the matrix M_ν^A , which do not contribute at tree level to neutrino masses. It is therefore quite easy to arrange the magnitude of the mass splitting at will, and this without disturbing the IRFP, which does not depend on the overall magnitude of M_ν^A but only on the ratio of its elements [see Eq. (44)]. Note also that the global scale of M_ν^A , which is in principle an unknown in this kind of scenarios, is thus fixed to get the correct mass splitting. In conventional scenarios the latter is adjusted by tuning the initial mass splitting at high energy, as discussed in the previous section.

4.3 Atmospheric angle

As in the conventional cases, amplification of the atmospheric angle requires that T_{31} or T_{32} dominate the RGEs of the neutrino mixing angles [we will not discuss the case $T_{31} \simeq T_{32}$ which in this scenario seems an unnatural coincidence in view of Eq.(37)]. Both cases are in fact very similar, so we consider in some detail only the case of T_{31} -dominance and later explain what changes would apply to the other case. Incidentally, notice from (37) that a natural way to get $T_{31} \gg T_{21}$ is $|m_2 - m_1| \gg |m_3 - m_1|$, implying $m_1 \simeq -m_2 \simeq m_3$, as for the conventional case.

If T_{31} dominates the evolution of the angles, the column $V_{\alpha 2}$ does not change much and should be chosen to agree with experimental data. This is imposed by hand as an initial condition, to be explained by physics at higher energy scales. By unitarity, this requirement amounts to only two conditions on the mixing angles. The IRFP is determined as usual by the condition $T_{31} \rightarrow 0$, which leads to the third condition on the mixing angles:

$$(c_1 c_3 c_{2\theta_2} + s_1 s_2 s_3)m_{e\tau}^A \simeq c_2 (s_3 c_{2\theta_1} + s_2 s_{2\theta_1} c_3)m_{\mu\tau}^A . \quad (47)$$

This IRFP condition amounts to one prediction for the angles in these scenarios.

One interesting possibility for the IRFP is the following. If $m_{e\tau}^A \ll m_{\mu\tau}^A$ the IRFP (47) reads $\tan 2\theta_1 \rightarrow -s_3/(s_2 c_3)$. This correlation between angles relates the smallness

of the CHOOZ angle to the maximality of the atmospheric one and can be taken as an interesting prediction of this particular scenario.

The case of T_{32} -dominance is obtained from the previous one by the replacement $c_3 \rightarrow s_3$ and $s_3 \rightarrow -c_3$ (which interchanges the first and second columns of V). The IRFP condition is then

$$(c_1 s_3 c_{2\theta_2} + s_1 s_2 c_3) m_{e\tau}^A \simeq c_2 (-c_3 c_{2\theta_1} + s_2 s_{2\theta_1} s_3) m_{\mu\tau}^A, \quad (48)$$

and all implications that follow are quite similar to the ones discussed above.

As for the solar case, provided the running reaches the IRFP, the low-energy mass splitting Δm_{13}^2 is of purely radiative origin and given by an expression similar to (46). Again the global magnitude of M_ν^A can be chosen to reproduce the atmospheric splitting, without modifying the previous discussion of IRFPs for the atmospheric angle, which are just controlled by the ratios of M_ν^A entries [see Eqs. (47, 48)]. Furthermore, in contrast with the conventional cases discussed in Sect. 3.3, this is achieved without upsetting the solar mass splitting. To see this notice that $m_1 \simeq -m_2 \simeq \pm m_3$ implies that the radiative correction to the solar splitting, still given by Eq.(46), is now of the order $\delta_{RG} \Delta m_{sol}^2 \sim \Delta m_{atm}^2 \Delta m_{sol}^2 / m^2$.

5 Conclusions

The nearly bi-maximal structure of the neutrino mixing matrix, V_{PMNS} , is very different from that of V_{CKM} in the quark sector, where all the mixings are small. An attractive possibility to understand this is that some neutrino mixings are radiatively enhanced, i.e. are initially small and get large in the RG running from high to low energy.

In this paper we have carefully examined this issue in two different contexts: conventional scenarios, in particular the SM and the MSSM, and supersymmetric scenarios in which neutrino masses originate in the Kähler potential. The RGEs are quite different in each case, and so are the results and conclusions. Our analysis is complete in the sense that we have taken into account all neutrino parameters, to ensure that not only mixing angles but also mass splittings agree with experiment at low energy. Moreover we have investigated which scenarios require a fine-tuning in order to achieve the amplification, and quantified it. In order to explain in an intuitive way the main issues involved in the running (appearance of infrared fixed points, interplay between

the running of the angles and that of the mass splittings, origin of the fine-tunings, etc.) we have first studied the two-flavour scenario, where all these features show up in a transparent way. Then, we have explored the physical cases exhaustively. Our main results and conclusions are the following.

- In the SM it is not possible to amplify either the solar or the atmospheric mixings, even with fine-tunings. Simply, the radiative effects that modify the mixings (which are proportional to the tau Yukawa coupling squared, y_τ^2) are not large enough to do the job for the currently preferred range of masses ($m \leq 0.3$ eV). For the same reason, the mass splittings cannot have a radiative origin.
- For the MSSM the amplification is possible but only when (at least two) neutrinos are quasi-degenerate (in absolute value and sign), and always involves a fine-tuning between the initial mass splitting (solar or atmospheric) and its radiative correction: two physically unrelated quantities that are required to be close to each other. The magnitude of this fine-tuning is essentially the amplification factor achieved. Moreover, a precise value of $\tan\beta$ (very high for the atmospheric case) is required. The amplification of the atmospheric angle requires an additional and even more important fine-tuning, since the solar splitting gets a radiative correction of “atmospheric” size which should be compensated by an ad-hoc initial condition. Finally, simultaneous amplification of solar and atmospheric angles is possible but it is extremely fine-tuned.

All these problems come from the fact that in the SM and the MSSM the mixing matrix (when there is some initial quasi-degeneracy) approaches an infrared pseudo-fixed-point (IRFP) which implies a physically unacceptable mixing (solar or atmospheric). Therefore, parameters should be delicately chosen for the running to stop before reaching the IRFP.

- Things are much better for the scenario of neutrino masses arising from the Kähler potential. First of all, the infrared fixed points correspond here to maximal or quasi-maximal mixings, so there is no need of fine-tuning in order to amplify angles. This can work for both the solar and the atmospheric angles.

Moreover, the amplification mechanism can work even if the mass eigenvalues are not quasi-degenerate. The reason is that the strength of the RG effect is

proportional to $m^A/(m_i - m_j)$, where m^A is the scale of a coupling that arises from the Kähler potential and m_i are the mass eigenvalues [in conventional cases the strength of the effect is proportional to $(m_i+m_j)/(m_i-m_j)$]. So it is enough to have $m^A \gg m_i - m_j$ to get important radiative effects, thus reaching the IRFP. On the other hand, the presence of m^A introduces an additional uncertainty, which is however removed taking into account that here the low-energy splitting, Δm_{ij}^2 , is essentially a pure radiative effect, whose magnitude can be adjusted with the value of m^A without modifying the form of the IRFP.

We find very encouraging that the scenario of neutrino masses from the Kähler potential, which is attractive for different reasons (e.g. it implies that the scale of lepton number violation is much closer to the electroweak scale than in conventional scenarios) has this remarkable and nice behaviour regarding radiative corrections.

To conclude, two more comments are in order. First, radiative effects play a relevant role in neutrino physics that often cannot be ignored. E.g. in view of the scarce success of radiative amplification in the MSSM, one might think that radiative effects are not relevant for model building in that framework. However, especially for scenarios involving some quasi-degeneracy, radiative effects can have the (negative) effect of destabilizing the high-energy pattern of mixing angles and mass splittings. The formulae presented in this paper are useful to analyze these effects. Second, the radiative corrections studied in this paper are model-independent since they concern the running from the M -scale (the scale where the new physics that violates L appears) down to the electroweak scale and this running is determined by the effective theory valid in that range (the SM or the MSSM with a non-renormalizable operator responsible for neutrino masses). Besides these corrections there are others arising from physics beyond M ,¹² but they are much more model-dependent. Their role is to set the initial conditions at M for the model-independent radiative effects analyzed here.

¹²E.g. threshold corrections at M or corrections from the running between a fundamental scale, say M_P or M_{GUT} , and M . In the see-saw model this corresponds to the running of the neutrino Yukawa couplings, Y_ν , and the right-handed neutrino masses between M_P and M . These effects can be quite important (for the see-saw they depends on the magnitude of Y_ν and have been analyzed elsewhere [28,49]).

A. RGEs for neutrino physical parameters

The energy-scale evolution of a 3×3 neutrino (Majorana) mass matrix \mathcal{M}_ν is generically described by a RGE of the form ($t = \log Q$):

$$\frac{d\mathcal{M}_\nu}{dt} = -(u\mathcal{M}_\nu + P\mathcal{M}_\nu + \mathcal{M}_\nu P^T) , \quad (\text{A.1})$$

In (A.1), u is a number, so $u\mathcal{M}_\nu$ gives a family-universal scaling of \mathcal{M}_ν which does not affect its texture, while P is a matrix in flavour space thus producing a non family-universal correction (the most interesting effect).

As explained in [30] one can extract from (A.1) the RGEs for the physical neutrino parameters: the mass eigenvalues, the mixing angles and the CP phases. In this paper we focus for simplicity on real cases, with no phases. (General formulas for the case with all phases can be found in [30].) Using the parametrization and conventions of the Introduction, we get the following RGEs for the mass eigenvalues and the PMNS matrix

$$\frac{dm_i}{dt} = -um_i - 2m_i \hat{P}_{ii} , \quad (\text{A.2})$$

$$\frac{dV}{dt} = VT . \quad (\text{A.3})$$

We have defined

$$\hat{P} \equiv \frac{1}{2} V^T (P + P^T) V , \quad (\text{A.4})$$

while T is a 3×3 matrix (anti-hermitian, so that the unitarity of V is preserved by the RG running) with

$$\begin{aligned} T_{ii} &\equiv i\hat{Q}_{ii} , \\ T_{ij} &\equiv \nabla_{ij} \hat{P}_{ij} + i\hat{Q}_{ij} , \quad i \neq j , \end{aligned} \quad (\text{A.5})$$

where

$$\hat{Q} \equiv \frac{i}{2} V^T (P - P^T) V , \quad (\text{A.6})$$

and

$$\nabla_{ij} \equiv \frac{m_i + m_j}{m_i - m_j} . \quad (\text{A.7})$$

Note that the RGE for V does not depend on the universal factor u , as expected.

From eqs. (A.3–A.7), we can derive the general RGEs for the mixing angles:

$$\frac{d\theta_1}{dt} = \frac{1}{c_2} (s_3 T_{31} - c_3 T_{32}) , \quad (\text{A.8})$$

$$\frac{d\theta_2}{dt} = - (c_3 T_{31} + s_3 T_{32}) , \quad (\text{A.9})$$

$$\frac{d\theta_3}{dt} = -\frac{1}{c_2} T_{21} + \frac{s_2}{c_2} (s_3 T_{31} - c_3 T_{32}) . \quad (\text{A.10})$$

In the next subsections we particularize the generic formulas above to scenarios of interest: first to the Standard Model and the MSSM and then to models with more sources of lepton number violation, among them supersymmetric scenarios with neutrino masses that are generated from the Kähler potential.

Conventional SM and MSSM

In the SM or the MSSM the RGE for the neutrino mass matrix (7) is of the form (A.1). The evolution of neutrino masses is then given by (no sum in i)

$$\frac{dm_i}{dt} = -u_M m_i - 2m_i c_M \hat{P}_{Eii} , \quad (\text{A.11})$$

where $\hat{P}_E = V^T P_E V$ and $P_E \equiv Y_E Y_E^\dagger / (16\pi^2)$ with Y_E the matrix of leptonic Yukawa couplings, which can be well approximated by $Y_E \simeq \text{diag}(0, 0, y_\tau)$ so that $16\pi^2 \hat{P}_{Eij} \simeq y_\tau^2 V_{\tau i} V_{\tau j}$. The model-dependent quantities u_M and c_M are as follows [24]–[27]. In the SM

$$u_M \simeq \frac{1}{16\pi^2} [3g_2^2 - 2\lambda - 6h_t^2] , \quad (\text{A.12})$$

where g_2, λ, h_t are the $SU(2)$ gauge coupling, the quartic Higgs coupling and the top-Yukawa coupling (leptonic Yukawa couplings can be safely neglected here), while in the MSSM

$$u_M = \frac{1}{16\pi^2} \left[\frac{6}{5} g_1^2 + 6g_2^2 - 6 \frac{h_t^2}{\sin^2 \beta} \right] , \quad (\text{A.13})$$

where g_1 is the $U(1)$ gauge coupling and $\tan \beta$ is the ratio of the vevs of the two supersymmetric Higgses. Finally,

$$c_M = \frac{3}{2} \quad (\text{SM}) , \quad c_M = -1 \quad (\text{MSSM}) . \quad (\text{A.14})$$

The RGE for the mixing matrix is of the form (A.3) with

$$\begin{aligned} T_{ii} &= 0 , \\ T_{ij} &= c_M \nabla_{ij} \hat{P}_{Eij} \simeq \epsilon_\tau \nabla_{ij} V_{\tau i} V_{\tau j} , \quad i \neq j , \end{aligned} \quad (\text{A.15})$$

with

$$\epsilon_\tau \equiv c_M \frac{y_\tau^2}{16\pi^2} , \quad (\text{A.16})$$

where electron and muon Yukawa couplings have been neglected. The running of the mixing angles, Eqs. (A.8–A.9), is now given by ($s_i \equiv \sin \theta_i$, etc)

$$\frac{d\theta_1}{dt} = -\epsilon_\tau c_1 (-s_3 V_{\tau 1} \nabla_{31} + c_3 V_{\tau 2} \nabla_{32}) , \quad (\text{A.17})$$

$$\frac{d\theta_2}{dt} = -\epsilon_\tau c_1 c_2 (c_3 V_{\tau 1} \nabla_{31} + s_3 V_{\tau 2} \nabla_{32}) , \quad (\text{A.18})$$

$$\frac{d\theta_3}{dt} = -\epsilon_\tau (c_1 s_2 s_3 V_{\tau 1} \nabla_{31} - c_1 s_2 c_3 V_{\tau 2} \nabla_{32} + V_{\tau 1} V_{\tau 2} \nabla_{21}) . \quad (\text{A.19})$$

More general models

Consider now a 3×3 neutrino mass matrix \mathcal{M}_ν that evolves with energy following a RGE of the form

$$\frac{d\mathcal{M}_\nu}{dt} = -(u_M \mathcal{M}_\nu + c_M P_E \mathcal{M}_\nu + c_M \mathcal{M}_\nu P_E^T) + P_E M_\nu^A - M_\nu^A P_E^T, \quad (\text{A.20})$$

where, besides the usual terms there are new contributions coming from M_ν^A , a 3×3 antisymmetric matrix that arises from lepton-violating physics but is not directly related to neutrino masses. Particular examples of RGEs of this form have been considered in the literature [40,46,60].

The explicit RGEs for neutrino mass eigenvalues, m_i , and mixing matrix, $V_{\alpha i}$, presented above for generic models with no M_ν^A -terms [Eqs. (A.2) and (A.3)] can be immediately extended also to Eq. (A.20) simply making the substitution

$$P \rightarrow c_M P_E - P_E M_\nu^A \mathcal{M}_\nu^{-1} , \quad (\text{A.21})$$

which transforms (A.1) into (A.20). More explicitly, we obtain (no sum in i)

$$\frac{dm_i}{dt} = -u_M m_i - \frac{y_\alpha^2}{8\pi^2} [c_M m_i V_{\alpha i}^2 - V_{\alpha i} m_{\alpha\beta}^A V_{\beta i}] , \quad (\text{A.22})$$

and the usual

$$\frac{dV}{dt} = VT , \quad (\text{A.23})$$

with T given by

$$T_{ii} = 0 ,$$

$$16\pi^2 T_{ij} = c_M y_\alpha^2 V_{\alpha i} V_{\alpha j} \nabla_{ij} - (y_\alpha^2 - y_\beta^2) \frac{V_{\alpha i} V_{\beta j}}{m_i - m_j} m_{\alpha\beta}^A . \quad (\text{A.24})$$

The explicit RGEs for the mixing angles, Eqs. (A.8–A.10), are also valid in this case upon substitution of T_{ij} as above.

If we particularize these results to a case with just 2 flavors (α, β), with mass eigenvalues $m_{1,2}$ and a single mixing angle θ ($V_{\alpha 2} \equiv \sin \theta$) we obtain the RGE (no sum in α, β)

$$16\pi^2 \frac{d\theta}{dt} = \frac{(y_\alpha^2 - y_\beta^2)}{m_1 - m_2} \left[\frac{c_M}{2} (m_1 + m_2) \sin 2\theta - m_{\alpha\beta}^A \cos 2\theta \right]. \quad (\text{A.25})$$

From this equation we deduce the following. When M_ν^A is absent, there is an infrared pseudo-fixed point at $\theta^* = 0, \pi/2$ in the evolution of θ . This is the case in most scenarios usually considered, for example the SM and the MSSM (with neutrino masses obtained from the superpotential). On the other extreme case, with $c_M=0$ and M_ν^A present, the pseudo-fixed point is at maximal mixing, $\theta^* = \pi/4$. The only instance that we know of such case is the MSSM with neutrino masses obtained through the Kähler potential [46] that we have considered in this paper. In cases with both c_M and M_ν^A non-zero, the pseudo-fixed point is at

$$\tan 2\theta^* = \frac{2c_M m_{\alpha\beta}^A}{m_1 + m_2}. \quad (\text{A.26})$$

This latter case can be realized for instance in non-supersymmetric two Higgs doublet models and has been studied previously in Ref. [60]. Note however that the analysis of fixed points in that reference is different from ours: in [60] it is assumed that neutrino masses also reach their fixed points, which is not usually the case in most examples of phenomenological interest. On the other hand, mixing angles quickly evolve to the fixed point if there is quasi-degeneracy of neutrino masses (with same sign masses, see e.g. the extended discussion in [30]).

B. RGEs for couplings in the Kähler potential

For a tree-level Kähler potential

$$K = \sum_a |\phi_a|^2 + \frac{1}{2M} \left[\kappa_c^{ab} \phi_a \phi_b \phi_c + \text{h.c.} \right] + \frac{1}{4M^2} \kappa_{cd}^{ab} \phi_a \phi_b \phi_c \phi_d + \frac{1}{6M^2} \left[\kappa_d^{abc} \phi_a \phi_b \phi_c \phi_d + \text{h.c.} \right], \quad (\text{B.1})$$

(with $\phi^a \equiv \phi_a^*$) and a superpotential that includes the Yukawa couplings

$$W = \dots + \frac{1}{3!} Y^{abc} \phi_a \phi_b \phi_c, \quad (\text{B.2})$$

one gets, from the condition $dK/dt = 0$ and using the one-loop corrected expression for non-renormalizable Kähler potentials computed in Ref. [64], the RGEs

$$16\pi^2 \frac{d\kappa_c^{ab}}{dt} = \left[\frac{1}{2} \kappa_c^{ax} Y^{bmn} Y_{xmn} + 2\kappa_y^{ax} Y^{ymb} Y_{xmc} + (b \leftrightarrow a) \right] + \frac{1}{2} \kappa_x^{ab} Y^{xmn} Y_{cmn} - 2g_A^2 \kappa_c^{ab} \left[C_2^A(a) + C_2^A(b) - C_2^A(c) \right] , \quad (\text{B.3})$$

$$16\pi^2 \frac{d\kappa_d^{abc}}{dt} = \left[\frac{1}{2} \kappa_d^{abx} Y^{cmn} Y_{xmn} + 2\kappa_y^{abx} Y^{cym} Y_{dxm} - \frac{4}{3} \kappa_x^{an} \kappa_y^{bm} Y^{yxc} Y_{nmd} - \frac{4}{3} \kappa_x^{an} \kappa_n^{by} Y^{mxc} Y_{myd} - \frac{4}{3} \kappa_x^{bn} \kappa_n^{ay} Y^{mxc} Y_{myd} + (bca) + (cab) \right] + \frac{1}{2} \kappa_x^{abc} Y^{xmn} Y_{dmn} - 2g_A^2 \kappa_d^{abc} \left[C_2^A(a) + C_2^A(b) + C_2^A(c) - C_2^A(d) \right] , \quad (\text{B.4})$$

$$16\pi^2 \frac{d\kappa_{cd}^{ab}}{dt} = \frac{1}{2} \left[\kappa_{cd}^{xb} Y^{amn} Y_{xmn} + (a \leftrightarrow b) \right] + \frac{1}{2} \left[\kappa_{xd}^{ab} Y^{xmn} Y_{cmn} + (c \leftrightarrow d) \right] + 2 \left\{ \left[\kappa_{yd}^{xb} Y^{amy} Y_{xmc} - \kappa_j^{am} \kappa_{ck}^n Y^{jkb} Y_{mnd} - \kappa_j^{am} \kappa_{cm}^n Y^{jkb} Y_{knd} - \kappa_j^{am} \kappa_{cn}^j Y^{nkb} Y_{kmd} + (c \leftrightarrow d) \right] + (a \leftrightarrow b) \right\} + 4g_A^2 \left[\kappa_{xy}^{ab} (T_{A\alpha})_c^x (T_{A\alpha})_d^y + \kappa_{cd}^{xy} (T_{A\alpha})_x^a (T_{A\alpha})_y^b \right] , \quad (\text{B.5})$$

where $C_2^A(a)$ is the quadratic Casimir invariant of the chiral field ϕ_a for the gauge group labelled by A (with gauge coupling g_A), and the $T_{A\alpha}$'s are the group generators (with A labelling the group and α the generator). The diagrammatic techniques of [65] were useful to compute the non-abelian gauge contributions to these equations. If the superpotential contains mass terms $\mu^{ab} \phi_a \phi_b$ with $\mu^{ab} \sim \mathcal{O}(\mu)$, the previous RGEs would receive additional contributions (*e.g.* terms like $\kappa_c^{ax} \kappa_{xz}^y \mu_{ry} Y^{zrb}$ in the RGE of κ_c^{ab}) proportional to μ/M . We neglect them on the assumption that $\mu/M \ll 1$.

References

- [1] B. Pontecorvo, Sov. Phys. JETP **26** (1968) 984 [Zh. Eksp. Teor. Fiz. **53** (1967) 1717]; Z. Maki, M. Nakagawa and S. Sakata, Prog. Theor. Phys. **28** (1962) 870.
- [2] C. Athanassopoulos *et al.* [LSND Collaboration], Phys. Rev. Lett. **77** (1996) 3082 [nucl-ex/9605003]; Phys. Rev. C **58** (1998) 2489 [nucl-ex/9706006]; Phys. Rev. Lett. **81** (1998) 1774 [nucl-ex/9709006].
- [3] S. Weinberg, Phys. Rev. Lett. **43** (1979) 1566.
- [4] T. Yanagida, procs. of the Workshop on Unified Theories and Baryon Number in the Universe, Tsukuba, Japan 1979 (eds. O. Sawada and A. Sugamoto, KEK Report No. 79-18, Tsukuba); S.L. Glashow, procs. of Quarks and Leptons, Cargèse 1979 (eds. M. Lévy *et al.*, Plenum, New York); M. Gell-Mann, P. Ramond and R. Slansky, procs. of the Supergravity Stony Brook Workshop, New York, 1979, (eds. P. Van Nieuwenhuizen and D. Freedman, North-Holland, Amsterdam); R. N. Mohapatra and G. Senjanovic, Phys. Rev. Lett. **44** (1980) 912.
- [5] L. Wolfenstein, Phys. Rev. D **17** (1978) 2369; S. P. Mikheev and A. Y. Smirnov, Sov. J. Nucl. Phys. **42** (1985) 913 [Yad. Fiz. **42** (1985) 1441]; Nuovo Cim. C **9** (1986) 17.
- [6] M. C. González-García and C. Peña-Garay, [hep-ph/0306001].
- [7] M. H. Ahn *et al.* [K2K Collaboration], Phys. Rev. Lett. **90** (2003) 041801 [hep-ex/0212007].
- [8] M. Apollonio *et al.* [CHOOZ Collaboration], Phys. Lett. B **466** (1999) 415 [hep-ex/9907037].
- [9] K. Eguchi *et al.* [KamLAND Collaboration], Phys. Rev. Lett. **90** (2003) 021802 [hep-ex/0212021].
- [10] Y. Fukuda *et al.* [Super-Kamiokande Collaboration], Phys. Lett. B **433** (1998) 9 [hep-ex/9803006]; Phys. Lett. B **436** (1998) 33 [hep-ex/9805006]; Phys. Lett. B **467** (1999) 185 [hep-ex/9908049]; Phys. Rev. Lett. **82** (1999) 2644 [hep-ex/9812014].

- [11] M. Ambrosio *et al.* [MACRO Collaboration], Phys. Lett. B **517** (2001) 59 [hep-ex/0106049]; M. Goodman, *XXth International Conference on Neutrino Physics and Astrophysics*, Munich May 2002. (<http://neutrino2002.ph.tum.de>).
- [12] D. A. Petyt [SOUDAN-2 Collaboration], Nucl. Phys. Proc. Suppl. **110** (2002) 349.
- [13] Y. Fukuda *et al.* [Kamiokande Collaboration], Phys. Rev. Lett. **77** (1996) 1683.
- [14] S. Fukuda *et al.*, Phys. Lett. B **539** (2002) 179 [hep-ex/0205075].
- [15] Q. R. Ahmad *et al.* [SNO Collaboration], Phys. Rev. Lett. **87** (2001) 071301 [nucl-ex/0106015]; Phys. Rev. Lett. **89** (2002) 011301 [nucl-ex/0204008].
- [16] B. T. Cleveland *et al.* [Homestake Collaboration], Astrophys. J. **496** (1998) 505.
- [17] J. N. Abdurashitov *et al.* [SAGE Collaboration], J. Exp. Theor. Phys. **95** (2002) 181 [Zh. Eksp. Teor. Fiz. **122** (2002) 211] [astro-ph/0204245].
- [18] W. Hampel *et al.* [GALLEX Collaboration], Phys. Lett. B **447** (1999) 127.
- [19] M. Altmann *et al.* [GNO Collaboration], Phys. Lett. B **490** (2000) 16 [hep-ex/0006034]; T. Kirsten, talk at the XXth International Conference on Neutrino Physics and Astrophysics (NU2002), Munich, (May 25-30, 2002).
- [20] H. V. Klapdor-Kleingrothaus *et al.* [Heidelberg-Moscow Exp.], Eur. Phys. J. A **12** (2001) 147 [hep-ph/0103062].
- [21] J. Bonn *et al.*, Nucl. Phys. Proc. Suppl. **110** (2002) 395.
- [22] O. Elgaroy *et al.* [2dFGRS], Phys. Rev. Lett. **89** (2002) 061301 [astro-ph/0204152].
- [23] D. N. Spergel *et al.* [WMAP Collaboration], [astro-ph/0302209].
- [24] P. H. Chankowski and Z. Pluciennik, Phys. Lett. B **316** (1993) 312 [hep-ph/9306333].
- [25] K. S. Babu, C. N. Leung and J. Pantaleone, Phys. Lett. B **319** (1993) 191 [hep-ph/9309223].
- [26] S. Antusch *et al.*, Phys. Lett. B **519** (2001) 238 [hep-ph/0108005]; Phys. Lett. B **525** (2002) 130 [hep-ph/0110366].

- [27] P. H. Chankowski and P. Wasowicz, *Eur. Phys. J. C* **23** (2002) 249 [hep-ph/0110237].
- [28] J. A. Casas, J. R. Espinosa, A. Ibarra and I. Navarro, *Nucl. Phys. B* **556** (1999) 3 [hep-ph/9904395]; *Nucl. Phys. B* **569** (2000) 82 [hep-ph/9905381].
- [29] J. A. Casas, J. R. Espinosa, A. Ibarra and I. Navarro, *JHEP* **9909** (1999) 015 [hep-ph/9906281]; R. Barbieri, G. G. Ross and A. Strumia, *JHEP* **9910** (1999) 020 [hep-ph/9906470].
- [30] J. A. Casas, J. R. Espinosa, A. Ibarra and I. Navarro, *Nucl. Phys. B* **573** (2000) 652 [hep-ph/9910420].
- [31] A. Ibarra and I. Navarro, *JHEP* **0002** (2000) 031 [hep-ph/9912282].
- [32] N. Haba, N. Okamura and M. Sugiura, *Prog. Theor. Phys.* **103** (2000) 367 [hep-ph/9810471]; N. Haba, Y. Matsui, N. Okamura and M. Sugiura, *Eur. Phys. J. C* **10** (1999) 677 [hep-ph/9904292]; *Prog. Theor. Phys.* **103** (2000) 145 [hep-ph/9908429]; N. Haba and N. Okamura, *Eur. Phys. J. C* **14** (2000) 347 [hep-ph/9906481]; N. Haba, Y. Matsui and N. Okamura, *Prog. Theor. Phys.* **103** (2000) 807 [hep-ph/9911481]; N. Haba, Y. Matsui, N. Okamura and T. Suzuki, *Phys. Lett. B* **489** (2000) 184 [hep-ph/0005064]; N. Haba, Y. Matsui and N. Okamura, *Eur. Phys. J. C* **17** (2000) 513 [hep-ph/0005075].
- [33] E. Ma, *J. Phys. G* **25** (1999) L97 [hep-ph/9907400]; R. Adhikari, E. Ma and G. Rajasekaran, *Phys. Lett. B* **486** (2000) 134 [hep-ph/0004197].
- [34] N. N. Singh, *Eur. Phys. J. C* **19** (2001) 137 [hep-ph/0009211].
- [35] T. K. Kuo, S. H. Chiu and G. H. Wu, *Eur. Phys. J. C* **21** (2001) 281 [hep-ph/0011058].
- [36] P. H. Chankowski, A. Ioannisian, S. Pokorski and J. W. Valle, *Phys. Rev. Lett.* **86** (2001) 3488 [hep-ph/0011150].
- [37] E. J. Chun, *Phys. Lett. B* **505** (2001) 155 [hep-ph/0101170].
- [38] M. C. Chen and K. T. Mahanthappa, *Int. J. Mod. Phys. A* **16** (2001) 3923 [hep-ph/0102215].

- [39] R. Gonzalez Felipe and F. R. Joaquim, JHEP **0109** (2001) 015 [hep-ph/0106226].
- [40] J. F. Oliver and A. Santamaria, Phys. Rev. D **65** (2002) 033003 [hep-ph/0108020].
- [41] S. Lavignac, I. Masina and C. A. Savoy, Nucl. Phys. B **633** (2002) 139 [hep-ph/0202086].
- [42] G. Bhattacharyya, A. Raychaudhuri and A. Sil, Phys. Rev. D **67** (2003) 073004 [hep-ph/0211074].
- [43] M. K. Parida, C. R. Das and G. Rajasekaran, [hep-ph/0203097].
- [44] G. Dutta, [hep-ph/0202097]; [hep-ph/0203222].
- [45] S. h. Chang and T. K. Kuo, Phys. Rev. D **66** (2002) 111302 [hep-ph/0205147].
- [46] J. A. Casas, J. R. Espinosa and I. Navarro, Phys. Rev. Lett. **89** (2002) 161801 [hep-ph/0206276].
- [47] A. S. Joshipura, S. D. Rindani and N. N. Singh, Nucl. Phys. B **660** (2003) 362 [hep-ph/0211378]; A. S. Joshipura and S. D. Rindani, Phys. Lett. B **494** (2000) 114 [hep-ph/0007334]; Phys. Rev. D **67** (2003) 073009 [hep-ph/0211404].
- [48] M. Frigerio and A. Y. Smirnov, [hep-ph/0212263].
- [49] S. Antusch, J. Kersten, M. Lindner and M. Ratz, Phys. Lett. B **538** (2002) 87 [hep-ph/0203233]; Phys. Lett. B **544** (2002) 1 [hep-ph/0206078]; S. Antusch and M. Ratz, JHEP **0211** (2002) 010 [hep-ph/0208136].
- [50] S. Antusch, J. Kersten, M. Lindner and M. Ratz, [hep-ph/0305273].
- [51] M. Tanimoto, Phys. Lett. B **360** (1995) 41 [hep-ph/9508247].
- [52] J. R. Ellis and S. Lola, Phys. Lett. B **458** (1999) 310 [hep-ph/9904279].
- [53] M. Carena, J. R. Ellis, S. Lola and C. E. Wagner, Eur. Phys. J. C **12** (2000) 507 [hep-ph/9906362].
- [54] J. R. Ellis, G. K. Leontaris, S. Lola and D. V. Nanopoulos, Eur. Phys. J. C **9** (1999) 389 [hep-ph/9808251].

- [55] P. H. Chankowski, W. Krolikowski and S. Pokorski, Phys. Lett. B **473** (2000) 109 [hep-ph/9910231]; P. H. Chankowski and S. Pokorski, Int. J. Mod. Phys. A **17** (2002) 575 [hep-ph/0110249].
- [56] K. R. Balaji, A. S. Dighe, R. N. Mohapatra and M. K. Parida, Phys. Rev. Lett. **84** (2000) 5034 [hep-ph/0001310]; Phys. Lett. B **481** (2000) 33 [hep-ph/0002177].
- [57] T. Miura, E. Takasugi and M. Yoshimura, Prog. Theor. Phys. **104** (2000) 1173 [hep-ph/0007066].
- [58] K. R. Balaji, R. N. Mohapatra, M. K. Parida and E. A. Paschos, Phys. Rev. D **63** (2001) 113002 [hep-ph/0011263].
- [59] T. K. Kuo, J. Pantaleone and G. H. Wu, Phys. Lett. B **518** (2001) 101 [hep-ph/0104131].
- [60] J. Pantaleone, T. K. Kuo and G. H. Wu, Phys. Lett. B **520** (2001) 279 [hep-ph/0108137].
- [61] R. N. Mohapatra, M. K. Parida and G. Rajasekaran, [hep-ph/0301234].
- [62] A. Zee, Phys. Lett. B **93** (1980) 389 [Erratum-ibid. B **95** (1980) 461]; P. H. Frampton and S. L. Glashow, Phys. Lett. B **461** (1999) 95 [hep-ph/9906375].
- [63] G. L. Fogli, E. Lisi and G. Scioscia, Phys. Rev. D **52** (1995) 5334 [hep-ph/9506350]; G. L. Fogli, E. Lisi and D. Montanino, Phys. Rev. D **54** (1996) 2048 [hep-ph/9605273].
- [64] A. Brignole, Nucl. Phys. B **579** (2000) 101 [hep-th/0001121].
- [65] P. Cvitanovic, Phys. Rev. D **14** (1976) 1536.